Local degradation of PEDOT:PSS on silicon nanostructures using scanning electrochemical microscopy

Yannick Dufil, Marc Dietrich, Dodzi Zigah, Frederic Favier, Saïd Sadki, Pascal Gentile, Olivier Fontaine

Local Degradation of PEDOT:PSS on Silicon Nanostructures Using Scanning Electrochemical Microscopy

Yannick Dufil[a], Marc Dietrich[b,c], Dodzi Zigah[c], Frederic Favier[a], Saïd Sadki[b], Pascal Gentile[c], and Olivier Fontaine[d]*

[a]ICGM, Univ Montpellier, CNRS, ENSCM, Montpellier, France.

[b] University Grenoble Alpes, CEA CNRS, Grenoble INP, IRIG-SyMMES, UMR 5819, Grenoble F-38000, France

[c] University Grenoble Alpes, CEA, Grenoble INP, IRIG-Pheliqs, Grenoble F-38000, France

[d]School of Energy Science and Engineering, Vidyasirimedhi Institute of Science and Technology (VISTEC), Rayong, 21210, Thailand.

[e]Institut Universitaire de France, 75005 Paris, France.

*Olivier Fontaine: olivier.fontaine@vistec.ac.th

Abstract

Conducting polymers show attractive characteristics as electrode materials for micro-electrochemical energy storage (MEES). However, there is a lack of characterization techniques to study conjugated/conducting polymer-based nanostructured electrodes. Here, scanning electrochemical microscopy (SECM) is introduced as a new technique for in situ characterization and acceleration of degradation processes of conducting polymers. Electrodes of PEDOT:PSS on flat silicon, silicon nanowires (SiNWs) and silicon nanotrees (SiNTrs) are analyzed by SECM in feedback mode with approach curves and chronoamperometry. The innovative degradation method using SECM reduces the time required to locally degrade polymer samples to a few thousand seconds, which is significantly shorter than the time usually required for such studies. The degradation rate is modeled using Comsol Multiphysics. The model provides an understanding of the phenomena that occur during degradation of the polymer electrode and describes them using a mathemat-ical constant A0 and a time constant τ.

1. Introduction

Conducting polymers are of growing interest as materials for micro-electrochemical energy storage devices.[1–3] This class of pseudocapacitive material are processed with low energy intensive processes offering a promising prospect for low fabrication cost and high flexibility.[4,5] Conducting polymers for application as electrodes and ionic conductors for solid state batteries and supercapacitors are one of the leading research topics in this field.[6,7]PEDOT:PSS is an attractive electrode material for supercapacitors among conducting polymers. It is one of the most widely used conducting polymers, shown to be of great significance for both fundamental research and large scale commercial research applications.[8] The main characteristic of supercapacitors, in addition to their outstanding power density, is a lifetime up to several hundreds of thousands of cycles. When cycled, under normal operating conditions, supercapacitors made of PEDOT:PSS exhibit satisfactory stability over a few thousand cycles[9–11] which is largely insufficient for commercial application. Recently, novel supercapacitor nanocomposite electrodes based on silicon nanostructures covered with PEDOT:PSS have shown an attractive increase of life spans[12]however, an

explanation for this increased stability is as yet to be provided, that is, degradation kinetics are of peculiar interest as they have a direct impact on the expected lifetime of a PEDOT:PSS supercapacitor electrodes. Until now, the main method used to investigate degradation consequences in conducting polymer films, and in PEDOT:PSS in particular, is to cycle them in operating conditions,[9,10] cycle them at overpotential and/or overheat to accelerate the degradation rate[13] or submit uncycled electrodes to UV radiation,[14] heat,[15,16] oxida-tive molecules[17] or humidity[18] over extended periods of time. A summary of the different electrode degradation techniques at multiple scales is given Figure1. The degradations techniques are detailed in Section S1, Supporting Information. The limitation with those large scale, full and half cells approaches is that it is difficult to obtain local data at the polymer scale. The second concern is that without extensive deviation from the nominal conditions of use, the degradation process will take from several weeks to several months. Scanning SECM provides access to the local electrochemical properties of the electrode under study. The local area affected directly depends on the size of the UltraMicroElectrode (UME) tip used. SECM has already been used to monitor Li-ion battery electrode degradation through in situ characterization of the solid electrolyte interface (SEI).[19] Cyclic voltammetry studies were made to characterize lithium (de)insertion on single LiMnO4 particles using SECM.[20] SECM in feedback mode has been used to study the kinetics of charge transfer between electrolyte and several conducting polymers: polyaniline,[21] polyalkylterthiophene,[22] polypyrrole,[23] or viologen-based polymers.[24] In this work, the charge transfer kinetics of electron from the redox mediator to the conducting polymer is linked to the apparent degradation state of the conducting polymer electrode. SECM is used in a very innovative way, as a tool for local analysis and accelerated degradation. This technique has the advantage, compared to conventional degradation methods, of locally degrading the electrode on a few square micrometers area. Thus, a single electrode can be used for multiple measurement points. It is also possible to access the local properties of the material where a classical approach gives us macroscopic information, being an advantage for nanocomposite characterization. The second advantage of this technique concerns the degradation conditions which are identical to the operational conditions found in a complete device. Finally, the analysis and the degradation are done in situ, using a single instrument. To our knowledge, this is the first ever study to use SECM as a mean of local and fast degradation for ageing purposes. SECM was first used in feedback mode to evaluate the kinetic parameters of the surface reaction of the redox mediator and the nanocomposite polymer electrode. This approximation was used to feed a finite element model of the SECM experiment using COMSOL Multiphysic software suite. The electrodes were then degraded using SECM in chronoamperometric mode to locally degrade the electrode in an accelerated way. Degradation characteristics of the electrodes were evaluated using the finite element model to infer the conducting polymer degrada-tion mechanism occurring on the different electrodes. Finally, the role of the electrode's microstructures is described and dis-cussed. Results reveal the great potential of SECM coupled with modeling as a complementary technique for the study and deg-radation of conducting polymers.

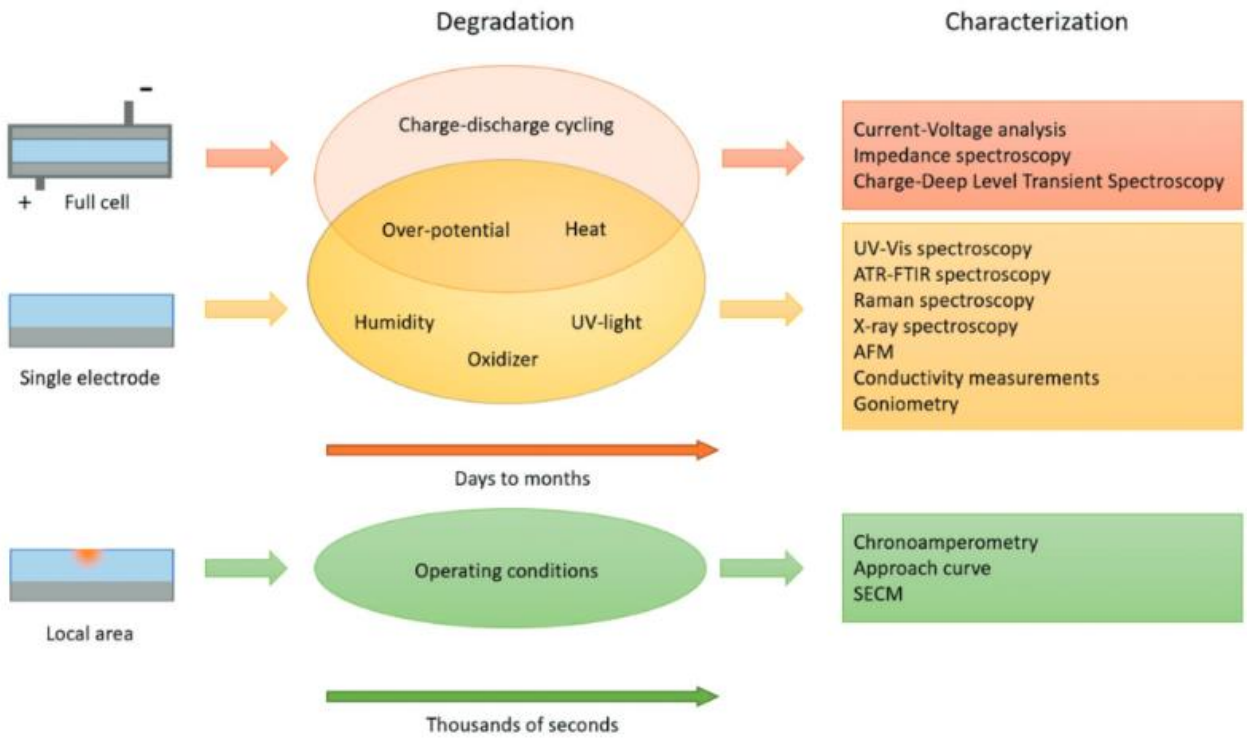

Figure1. Summary of the state-of-the-art techniques for PEDOT:PSS electrode degradation. Degradation and characterization techniques for each scale of electrodes. Full-cell detailed (in red), half cell (in orange), and this work with local scale through SECM (in green). Degradation step takes from several days to several months to proceed for full and half-cells whereas it takes only a few thousand seconds for local scale in this work.

2. Experimental Section

2.1. Electrolyte Preparation

Hexaammineruthenium(III) chloride was used as the redox mediator in an aqueous solution with Na2SO4 as sup-porting electrolyte. The concentration of [Ru(NH3)6]2+ was 1 × 10−3 mol L−1 and the concentration of supporting electrolyte 0.5 mol L−1. The solution was degassed for 1 min by nitrogen bubbling to prevent oxygen from interfering with the measure-ments. A flow of nitrogen was maintained on the surface of the solution during the whole duration of the experiments.

2.2. Modeling Scanning Electrochemical Microscopy

Models were built using COMSOL Multiphysics and are pre-sented Figure2. The model consists in a single domain which corresponds to the electrolyte, two external boundaries and four internal boundaries. Insulating conditions were placed on the two internal boundaries forming the interface between the electrolyte and the insulating part of the UME. Potentials were applied on the two boundaries forming the interfaces between the surface of both the UME and the nano-composite electrode with the electrolyte. Finally, to minimize computational needs, the model was built in 2D axisymmetric around the central axis of the UME.

A constant concentration constraint was set on the external boundaries with initial concentration values for both oxidized and reduced form of the redox shuttle. This in/outflux was meant to simulate the infinite supply of fresh solution to the vicinity of the UME. Transport was limited by diffusion only. In addition, no potential gradient was simulated in the solution, thanks to the presence of the supporting electrolyte.

Equation (1) emerges from those conditions to describe the solute concentration in the solution. Kinetics on both electrodes were driven by the Butler–Volmer equation (Equation (2)) and the equilibrium potential by the Nernst relation (Equation (3)). A triangular mesh was applied with a size constraint on the UME conductive surface of 0.5 µm maximum element size. The resulting mesh was comprised of between 1200 and 1800 elements of good quality (>0.78 skewness) depending of the tip-electrode distance (see Figure 2b).

$$\frac{\partial C_i}{\partial t} + \nabla \cdot \left(-D_i \nabla C_i\right) = R_i \tag{1}$$

$$i = i_0 \left(\exp\left(\frac{\alpha_a F \left(E_{eq} - E_{eq,ref}\right)}{RT} \right) - \exp\left(\frac{\alpha_c \left(E_{eq} - E_{eq,ref}\right)}{RT} \right) \right) \tag{2}$$

$$E_{eq} = E_{eq,ref}\,(T) - \frac{RT}{nF} ln \prod_i \left(\frac{C_i}{C_{i,ref}} \right)^{vi} \tag{3}$$

where Ci is the concentration of electrolyte (mol m−3), Di is the diffusion coefficient of the electrolyte (m2 s−1), Ri the reaction rate (mol m−1 s−1), i the current density (A cm−2), i0 the reference exchange current density (A cm−2), αa and αc the anodic and cathodic transfer coefficient, F is the Faraday's constant (s A mol−1), Eeq is equilibrium potential (V), Eeq,ref is the reference equilibrium potential (V) and R is the gas constant (J mol−1 K−1).

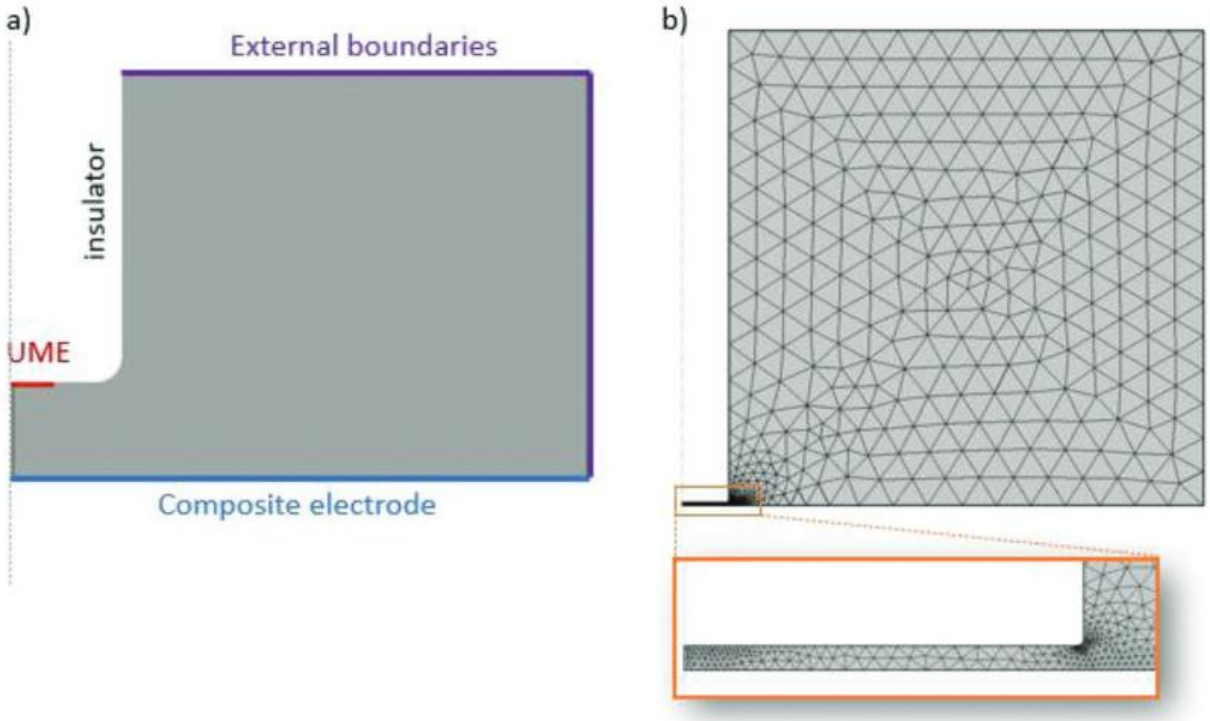

Figure2. Schematic representation of the SECM experiment. a) Simple model with the electrolyte domain represented in grey, the UME surface in red, the composite electrode surface in blue, the insulator around the UME in black, the external boundaries in purple, and the symmetry axe as a dashed grey line. b) On scale model with the applied mesh. A magnified view of the electrolyte under the UME is presented in the orange rectangle. The tip-electrode distance is here 1 µm.

3. Results and Discussion

3.1. Cyclic Voltammetry Experiments

Cyclic voltammetry was performed at the UME before each experiment between −0.45 and 0.1 V at 20 mV·s−1 with a platinum counter electrode and an Ag/AgCl reference elec-trode. The mass driven limit current was about −4.7 nA and the midpoint potential was −0.24 V. These observations are compatible with the standard potential of the [Ru(NH3)6]2+/[Ru(NH3)6]3+ couple −0.2 V versus SCE.[25] When the UME approaches the surface of the electrode, two phenomena compete: the diffusion of the redox mediator from the bulk and the regeneration of the electroactive species on the electrode. A schematic describing the concurring phenomena is given Figure3a. On the one hand, the diffusion of the redox mediator ions is more and more hindered by the insulator sur-rounding the UME.[23] This induces a decrease in the UME response current as less “fresh” electrolyte reach the surface of the electrode from the bulk. On the other hand, the proximity of the electrode to the UME shortens the distance the electrolyte

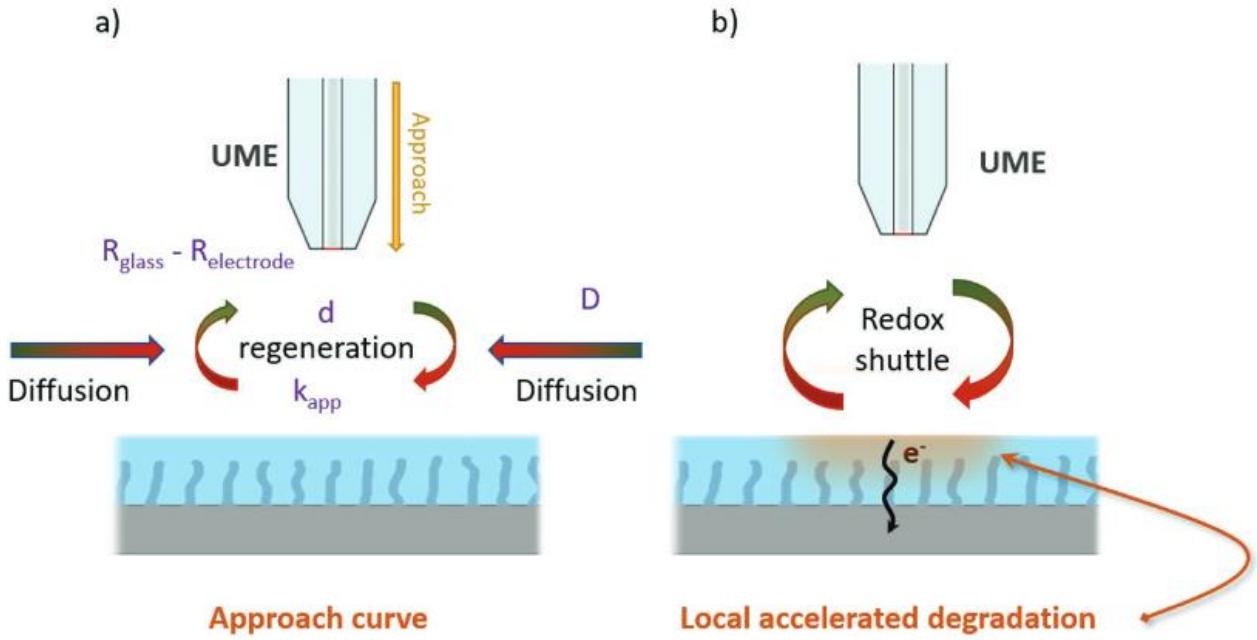

Figure3. Schematic of the SECM methods used. a) Approach curve. Red color on the arrows figures the oxidative state of the mediator while green figures the reduced state. b) Local accelerated degradation. The local accelerate degradation occurs directly under the UME

needs to travel to be regenerated, inducing an increase in the response current measured at the UME. The competition between the accelerated regeneration of the mediator at the electrode surface and the diffusion hindered by the proximity of the tip to the electrode is driven by the apparent rate constant kapp of the mediator regeneration at the UME surface. The response current is thus governed by five parameters: the radius of the UME a, the radius of the insulator surrounding the UME Rglass, the diffusion constant of the redox mediator D, the apparent rate constant kapp, and the distance between the UME and the electrode surface d. A series of steady state current computed at various distances between the electrode and the tip using the model allows us to build an approach curve. This approach curve is adapted to the approximations used by Cornut et al.,[26] and allows us to approximate the apparent time constant kapp.At a constant distance from the surface, the redox mediator undergoes a rapid oxidation–reduction cycle, bringing charges that locally and rapidly degrade the surface of the composite electrode. A schematic of the process is given in Figure 3b. As the composite electrode surface degrades, it becomes less efficient in regenerating the redox shuttle resulting in a diminution of the collected current at the tip of UME. The degradation time is then converted into equivalent cycles using the time it takes for the redox shuttle to diffuse between the UME and the composite electrode using Equation (4):

$$n_{\text{cycle}} = \frac{t_{\text{deg}}}{2 \times t_{\text{diff}}} \quad (4)$$ with

ncycle, the number of cycles equivalent to the degradation time (no unit), tdeg the total degradation time (in s), and tdiffthe time needed for the redox shuttle to diffuse from one elec-trode to the other (in s) (more details in Section S4, Supporting Information).

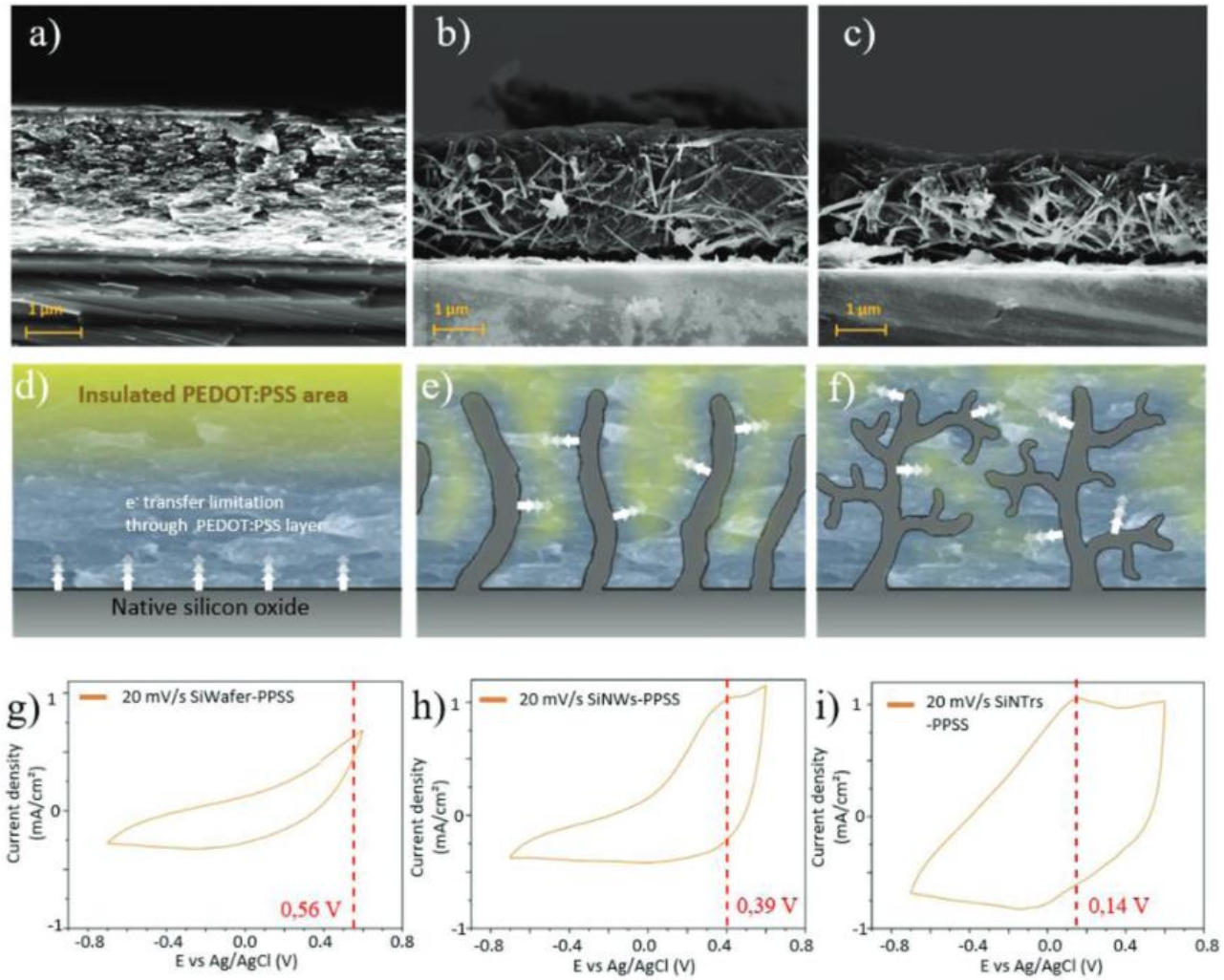

Figure4. Scanning electron microscopy cross-section view of the nano-composite electrodes. a) Silicon wafer and PEDOT-PSS, b) SiNWs and PEDOT-PSS and c) SiNTrs and PEDOT-PSS cross section view, showing the polymer covering the nanostructures, creating a Si grid inside of the polymeric matrix. d,g) On a flat silicon substrate, the polymer layer is virtually undoped in the area away from the electrode, which creates a charge gradient and slows the oxidation kinetics of the polymer. e,h) The presence of SiNWs decreases the thickness of undoped polymer, polymer oxidation peak occurs therefore earlier. f,i) With SiNTs, the undoped polymer thickness is further reduced, the polymer oxidation peak occurs at an even lower potential

3.2. Nanocomposite Electrodes Characteristics

The studied nano-composite electrodes were composed of a silicon electrode on the top of which is grown silicon nanostructures and chemically deposited PEDOT:PSS. The electrodes have been obtained by the method previously reported.[27–30]Corresponding scanning electron micrographs are presented Figure4a–f. Nanowires were produced by chemical vapor deposition (CVD), using the vapor–liquid–solid (VLS) method with a gold catalyst on highly doped n-silicon (111).[31] A second catalyst deposition on silicon nanowires allowed us to grow nanotree structures.[27,28] The polymer was then drop casted directly onto the nanostructures with ethanol as dispersing agent and dried overnight in a chemical hood.[12] Three different

nano-composite electrodes were studied with a variation in the type of nanostructures embedded in the PEDOT:PSS matrix. The first one (SiWafer) did not include nanostructures, as the polymer was deposited directly on planar silicon substrate. The polymer layer was 2.5 µm thick with a granular structure. The second one (SiNWs) included nanowires with diameters ranging from 20 to 200 nm for a length of 50 µm. The density of nanowires ranged from 2 × 107 to 2 × 108 SiNWs cm−2. The total thickness of the nano-composite electrode was 2.5 µm. The third one (SiNTrs) included nano trees with trunks diameters ranging from 20 to 200 nm for 50 µm length and branches with a diameter between 10 and 50 nm for 50 µm length and the same density as nanowires. The total thickness of the nano-composite electrode was 2 µm. Cyclic voltammetry (CV) of each electrode was performed at 20 mV s−1 with a platinum counter electrode and an Ag/AgCl reference electrode in aqueous Na2SO4 0.2 m. The SiWafer CV curve, presented in Figure 4g, shows the highest potential for the polymer oxida-tion peak. The SiNWs CV curve, presented in Figure 4h, shows a small shift toward lower potential for the polymer oxidation peak. The SiNTrs CV curve, presented in Figure 4i, shows the lowest potential for the polymer oxidation peak. We believe it is due to the electron transfer limitation trough the PEDOT layer, the effect of which is limited by the presence of nanostructures (Figure 4d–f). The global aspect of the CVs for the SiNTrs elec-trode is more resistive than for the SiNWs electrode, because of the oxidation of the many nanotrees apexes, forming insulating SiO2 areas.

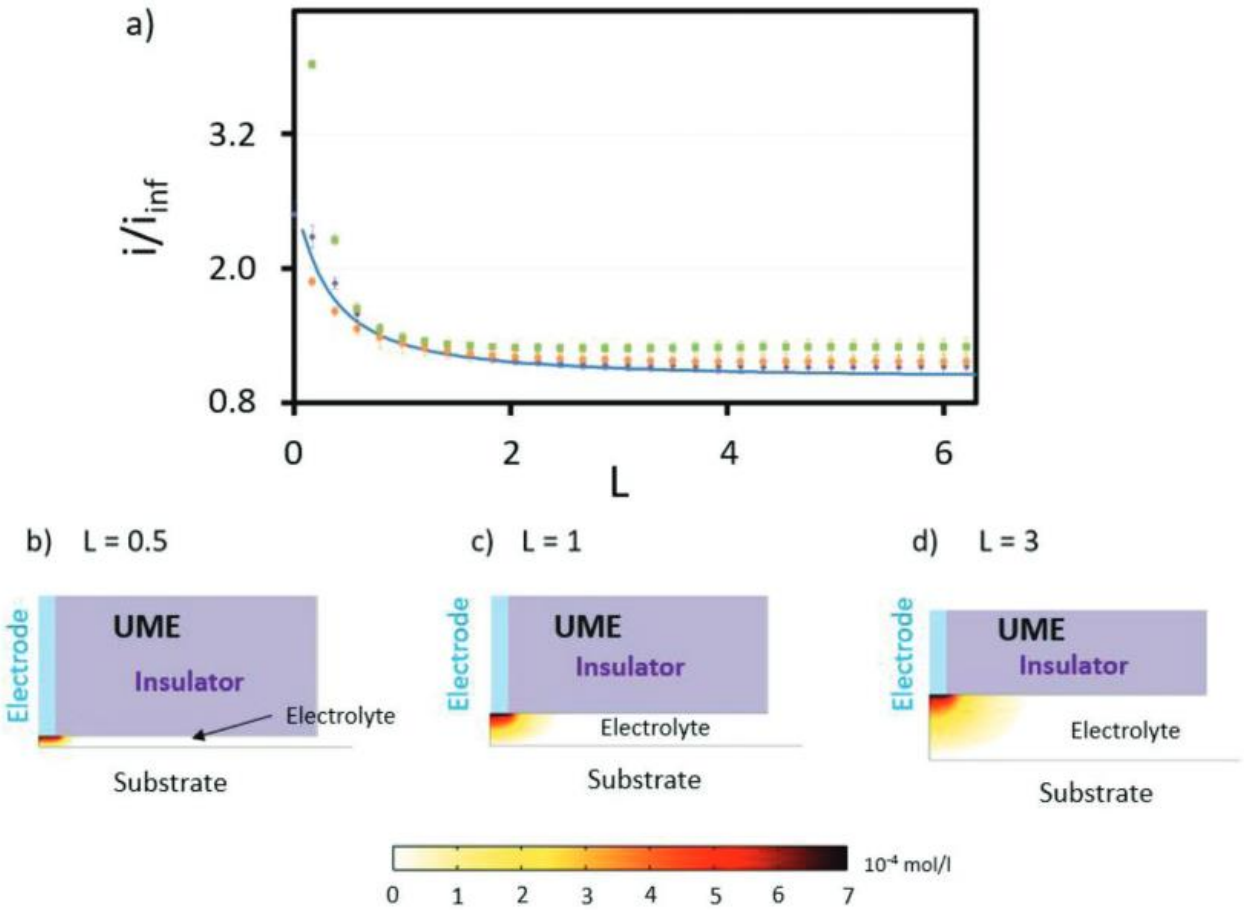

Figure5. SECM feedback mode results. a) Approach curves obtained from experiments (dot lines) on bare silicon (purple), SiNWs (orange), and SiNTrs (green) and from simulation (blue line) using our model on COMSOL. b–d) Visualization of the diffusion layer at different tip-electrode distance with L, ratio of the tip-electrode distance, and a radius of the electrode.

3.3. Composite Electrodes Display Similar Kinetic Constant

Approach curves were measured at multiple spots surface on the electrode and are presented Figure5a. The diffusion coefficient of [Ru(NH3)6]3+ ions in the solution was taken from literature at 8.4 × 10−10 m2 s−1.[32]

The five aforementioned parameters were used to calculate the approach curves using the Cornut et al.[26] method, which gave an estimation of the average apparent rate constant at 2.0 ± 0.3 10−4 m s−1 for the silicon-polymer electrode, 1.6 ± 0.2 10−4 m s−1 for the SiNTrs-polymer electrode and 4.6 ± 0.2 10−4 m s−1 for the SiNWs-polymer electrode. Giving the precision achievable with the used experimental set up, the reaction rate can be averaged for all three electrodes to 2.7 ± 1.6 10−4 m s−1 for the next step of this work. The fact that all three electrodes present similar reaction rates was expected. The reaction rate mainly depends of two parameters: the ion concentrations of the redox shuttle in the electrolyte and the concentration of electro-active sites on surface. The ion concentration in the electrolyte is identical for all experiments and the concentration of accessible p-doped PEDOT+ at the polymer electrolyte interface (see Equations (5) and (6) are independent of the presence of nanostructures within the polymer. Finally, the reaction rate value is comparable to that found in literature for other conductive polymers.[23]

$$\left[\mathrm{Ru(NH_3)_6}\right]^{2+} + \mathrm{PEDOT}^{+} \rightleftharpoons \left[\mathrm{Ru(NH_3)_6}\right]^{3+} + \mathrm{PEDOT} \quad (5)$$

$$\mathrm{PEDOT}^{+} \rightleftharpoons \mathrm{PEDOT} + e^{-} \quad (6)$$

$$\mathrm{PEDOT}^{+} \rightarrow \mathrm{PEDOT}_{\mathrm{DEAD}} \quad (7)$$

The electrode, by oxidizing the redox shuttle, captures an electron and transmits it to the current collector, thus mimicking the regular functioning of a pseudo-supercapacitor electrode. The redox shuttle diffuses to the UME to be regenerated, producing a feedback current during the process. The repetitive passages of electron through the electrode cause an irreversible chemical deactivation of the surface of the electrode as described by Equation (7). The number of chemically active sites, containing PEDOT+, on the surface of the electrode will decrease along with time. Given enough time, all the PEDOT+ that can be deactivated on the surface will follow and the electrode will reach the worst degradation state possible through chemical deactivation leading to the electrochemical performances capping. The feedback current generated at the UME depends on the physical parameters of the experiment and on a chemical variable. The physicals parameters are: tip-electrode distance, diffusion coefficient, insulator radius, and UME radius. The chemical variable is the apparent reaction time at the surface: kapp which is linked to the number of active PEDOT+ sites on the surface. The feedback current over time allows us to follow the evolution of the apparent reaction time constant at the electrode surface along time and thus the degradation state of the electrode. For each measurement, the electrode area impacted by degradation is of a few square micrometers. The tip-electrode distance for this process was set at 1 µm. Potential was 0.4 and −0.4 V versus Ag/AgCl at the UME and at the electrode respectively, to ensure a fast redox reaction. The degradation time is set to 5000 s which corresponds to ≈526 000 charge/discharge cycles equivalent.

3.4. Nano Wires Are More Stable and Nanotrees Degrade Faster

The electrodes were then degraded under the conditions described above. The apparent rate constant of the reaction at the surface of the electrode shows an exponential decrease with time. Such activity decreases have already been observed in the literature, for example, by Vitoratos et al.[17] They used a thermal degradation method where electrodes were heated to 120 °C for nearly 60 h. The conductivity of PEDOT:PSS was then meas-ured by the 4-probe method. The observation of the decrease in conductivity is a complement to the study of the chemical composition and electronic structure of the electrode by X-ray photoelectron spectroscopy (XPS) and ultraviolet photoelectron spectroscopy (UPS) that was performed.

The decay is usually assigned to the formation of PEDOT+clusters in the PSS− chains as depicted in Figure6a,b. Despite significantly different aging conditions, the mechanisms leading to cluster formation (i.e., the

disruption of hydrogen bonds ensuring cohesion between PEDOT+ and PSS−)[16] are concordant with electron injection into the polymer. The reaction rate constant follows an exponential decay law governed by two parameters: A0 and τ as described in Equation (8)

$$k_{app} = A_0 \cdot k_{0,sub} - (1 - A_0) \cdot k_{0,sub} \cdot \exp\left(-\frac{t}{\tau}\right) \quad (8)$$

with kapp the apparent reaction time constant (m s−1), A0 a mathematical parameter that quantifies the degradation intensity, k0,sub the initial reaction rate constant (m s−1), t the time (s), and τ an arbitrary time constant in (s).A0 is a mathematical constant related to the state of the con-ducting polymer surface after degradation. The A0 constant's value is comprised between 0 and 1. It can be viewed as what percentage of the reaction rate constant kapp remains at the end of the degradation. When A0= 0, zero percent of the reaction constant remains at the end of the degradation, resulting in an extremely low tip current at the end of the degradation. The tip current at the end of the degradation strictly results of the dif-fusion and is equal to the current observed for an insulating electrode. With the tip so close to the surface, such a tip current can be approximated as zero. On the other hand, when A0= 1, it means that 100% of the reaction time constant remains at the end of the degradation. The tip current doesn't decrease during degradation and stays constant over time. The degradation process is the same regardless of the value of A0. As the redox shuttle is regenerated on the surface of the composite electrode, the electrode is degraded and its local properties are modified. The number of regenerated redox molecules then decreases. Bülter et al.[19] have highlighted the passivation of their electrode by the formation of a solid electrolyte interphase (SEI) which hinders the regeneration of their redox shuttle. In their experiment, they scan the surface of their electrode at a constant height, that is, the tip-electrode distance is kept con-stant. From there, the variation of the feedback current can be attributed either to a different reactivity of the surface, or to the roughness of the electrode (bringing the surface closer to the tip). In the same way, we use the feedback current to investigate the surface condition of the electrode. However, we do not sweep the electrode surface with the tip, we hold it in place in order to locally degrade the electrode. In our case, only the number of electrochemically active sites varies upon time, which causes the decrease of the regeneration of the redox shuttle on the surface of the electrode and thus, the feedback current. τ is a time constant related to the kinetics of the deg-radation mechanisms that operates in the composite electrode. At t=τ, 63% of the max degradation has happened. At t= 3τ, 95% of the maximum degradation has happened. At t= 5τ, 99% of the maximum degradation has happened. Following that, the lower the value of τ, the faster the degradation kinetic. All parameters are summarized in Table1.

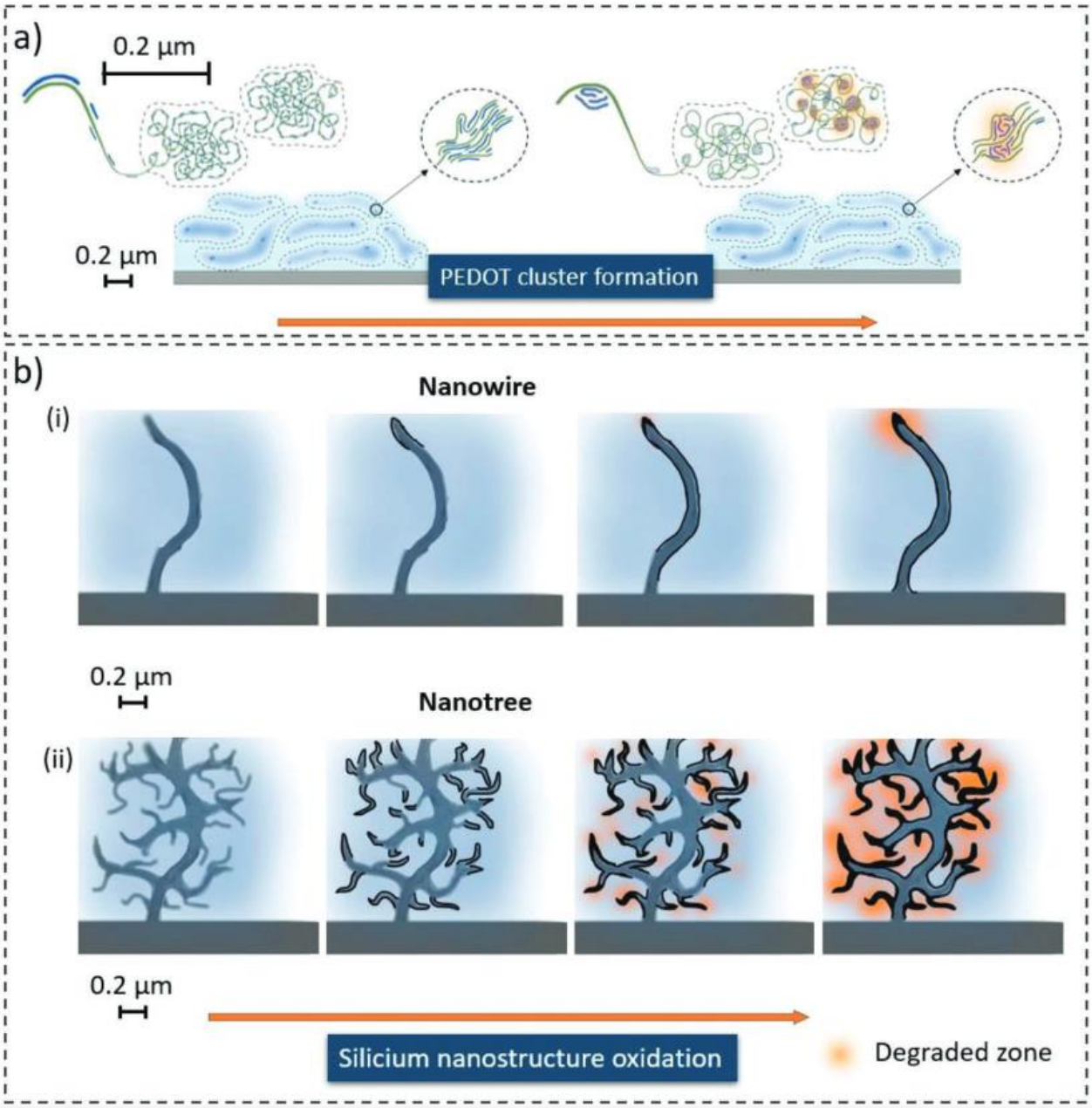

Figure6. Degradation mechanisms at work in nanocomposite polymer electrodes. a) PEDOT cluster formation with fresh polymer on the left and degraded polymer on the right. The granular structure of the polymer is detailed on top of each diagram. Cluster formation happens in all electrodes b) (i) SiNWs oxidation. The oxidation is logically believed to start at the tip and propagate along the nanowire b) (ii) SiNTrs oxidation. The oxidation is believed to start at the apex of the branches and growing to the center of them. At the end of the oxidation process, a large portion of the tree branches are totally oxidized and prevent conduction between electrode and polymer.

Electrode	D [$m^2\ s^{-1}$]	r_{glass} [µm]	$r_{electrode}$ [µm]	$K_{0,sub}$ [$m\ s^{-1}$]	A_0	τ [s]
SiWafer	8.4×10^{-10}	169	12.8	$2.0 \pm 0.3 \times 10^{-4}$	0.75 ± 0.05	125 ± 25
SiNws				$1.6 \pm 0.2 \times 10^{-4}$	0.93 ± 0.01	125 ± 25
SiNTrs				$4.6 \pm 0.2 \times 10^{-4}$	0.65 ± 0.07	30 ± 1
SiNTrs					$0.85 + 0.08$	1000 ± 70

Table1. Summary of parameter values for each electrode

In the present case, for the flat silicon PEDOT:PSS elec-trode, the parameter A0 was calculated at 0.75 ± 0.05, which is consistent with previous observations in the literature.[15] The parameter τ was calculated at 125 ± 25 s. This means that the degradation process is ending after about 625 s, which is very short compared to state-of-the-art degradation techniques (see Table2).Similar results were obtained for the degradation kinetic of SiNWs-PEDOT:PSS electrode with the same τ parameter as the Si-PEDOT:PSS electrode (Figure7a). This indicates that the kinetics of degradation in both electrodes are identical, which strongly suggests that the same degradation mechanism occurs with both electrodes during SECM local fast degradation. This is a surprising result because usually, 3D nanostructured electrodes have higher kinetic constants than flat silicon due to the high surface/volume ratio of SiNWs. Therefore, this proves that the degradation process probably occurs only in the polymer part of the electrode. However, the A0 parameter is significantly greater (0.93 ± 0.01) for the SiNWs-PEDOT:PSS electrode indicating an inhibiting effect of the nanowires on the degradation process. Degradation of PEDOT:PSS is described in the literature as a migration of PEDOT+ chains in the PEDOT:PSS matrix leading to insulated cluster formation (Figure 6a). These clusters are believed to shrink the conductive grains of the polymer matrix resulting in a decrease of its conductivity.[17] SiNWs, while not able to prevent the formation of these clusters, may inhibit the shrinking of the conductive grain of the polymer or bridge the grains, preventing the loss of conductivity.

Reference	Degradation method	Degradation stress	Degradation time
[18]	RH controlled resting	Underwater, 20% to 80% RH	180 days
[33]	Thermal	26 to 86 °C	120 days
[34]	Thermal, electrochemical	Nominal +10 °C, +200 mV	100 days
[35]	Resting	Dark, ≈22 °C, ≈55% RH	50 days
[15]	Thermal	25 to 200 °C	1000 h
[17]	Thermal	120 °C	55 h
This work	Electrochemical, local	Nominal	5000 s

Table2. Comparison of different PEDOT:PSS degradation technics.

The results for SiNTrs-PEDOT:PSS electrode degradation differ significantly from those obtained using the two previous electrodes as shown in Figure 7a. The degradation kinetics cannot be described with only a single exponential decay as there is a clear inflection about t= 1000 s. Adding a second exponential component allowed to better fit the experimental values and tended to demonstrate that two independent phe-nomena occur simultaneously during the degradation process. The first one can be described as abrupt with a τ constant of 30 ± 1 s and an A0 parameter of 0.65 ± 0.07. The second one is slower, even slower than for the first two samples with a τconstant of 1000 ± 70 s and a comparable shallowness as the SiNWs-PEDOT:PSS electrode with an A0 of 0.85 ± 0.08. Two parallel kinetics can be considered. One acts on the polymer while the other one acts on the SiNTrs. The fastest kinetics were assigned to the SiNTrs. Branches of the nano trees would suffer a passive form of oxidation in the aqueous electrolyte (Figure 6b-ii), forming insulating SiO2 layer which would sink down their conductivity and form large charge trapping areas. The same oxidation is

supposed to happen in the other two electrodes, however, the effect is significantly different. Diameters of the nanostructures are the critical parameter for oxidation effect on the electrode. The larger the diameter of the nanostructure, the lesser the effect of oxidation on the electrode. Nanowires possess larger diameters than the branches of nanotrees (Figure 6b-i,ii), hence the lesser effect of oxidation in silicon-nanostructure polymer electrodes. The slower kinetics were assigned to the polymer assuming that the PEDOT+ cluster formation is happening as it would with other electrodes. The decrease of the degradation kinetics is assigned to the density of the nanostructures that would slow down the shrinking of the conductive grains by either interfering with the migration of PEDOT+ inside the grain or physically maintaining the grain integrity. The latter is more likely than the former as the nanostructure size is of the same order of magnitude as the granular structure of the polymer.

4. Local Degradation by SECM Is Faster and Softer than State-of-the-Art Methods

State-of-the-art degradation techniques for PEDOT:PSS elec-trodes were studied and are summarized in Table 2. Classical degradation techniques consist in placing the samples in a con-trolled environment, close or not to their conditions of use, for an extended period of time. Degradation is therefore applied to the entire device or electrode. Different measurements are then conducted on the samples to quantify and qualify the different degradations that have taken place in the polymer. Among the techniques used, we can cite local probe microscopy (AFM, STM), spectrophotometry (UV, FTIR, RAMAN, X-RAY), or elec-trical measurements (conductivity, capacitance, impedance).

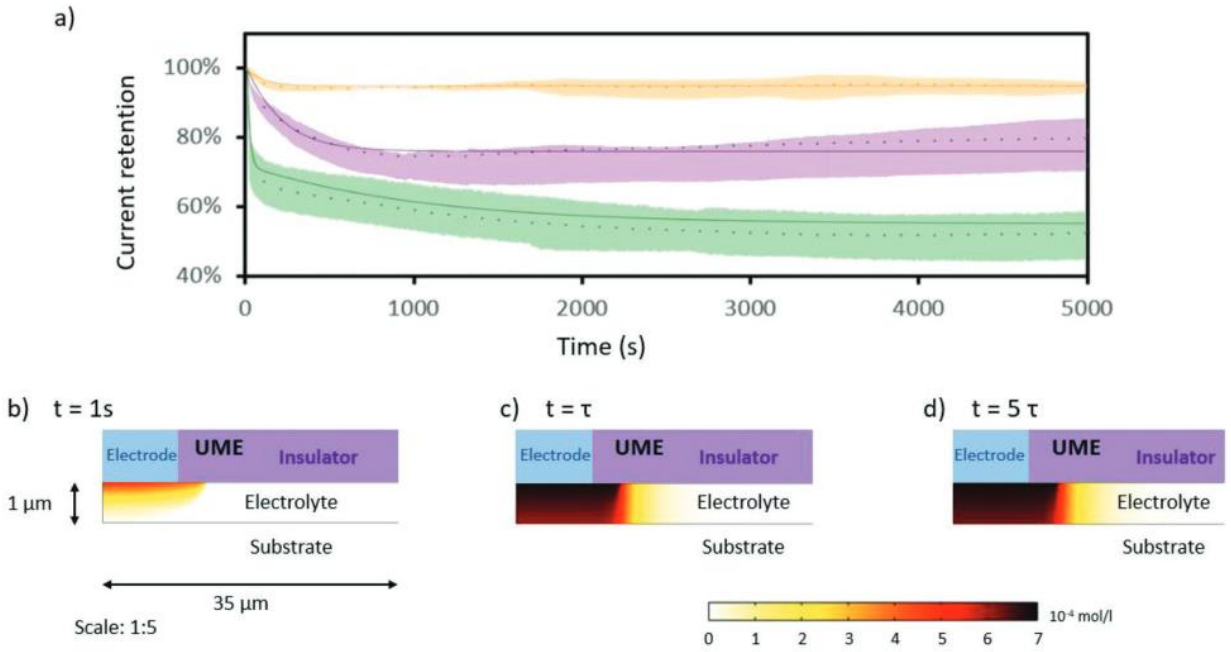

Figure7. Fast local degradation of nanocomposite electrodes. a) Experimental values (dots lines) and simulations (plain lines) of SiWafer (purple), SiNWs (orange), and SiNTrs (green). Tolerance is expressed by the shade around the dots. b–d) Diffusion layer of [Ru(NH3)6]2+ at different characteristic times of degradation. The color shows the diffusion layer of oxidated redox shuttle between the tip of the UME (blue) and the electrode.

SECM is a local technique. Contrary to the techniques discussed above, it is used to degrade and analyzes only a small part of the electrode, being relatively non-destructive while keeping multiple tests on a single sample. The microscopy reactivity access to local degradation phenomena is complementary to the previously mentioned degradation and characterization techniques. The other side of the coin is that previously mentioned analysis techniques cannot specifically be applied to the degraded area. When comparing the time required to degrade the elec-trodes, the SECM is more efficient than the commonly used

methods. The end of the degradation process is indeed reached in a few hundred to a few thousand seconds, while conventional methods require a few days to a few months. The stress applied to electrodes during degradation is very close to the conditions of use in the case of SECM. The temperature, relative humidity and potential, which are the factors commonly attributed to the degradation of PEDOT:PSS were chosen to match the nominal operating conditions of the electrode. On the other hand, state-of-the-art degradation techniques apply excessive stress to the electrodes to accelerate degradation. Finally, SECM as a degradation technique can only monitor the local electrochemical reactivity of the electrode. No direct information on chemical or structural alteration is collected, this limitation should be kept in mind when using this technique. We believe that these characteristics make SECM, used as a local technique, a valuable addition to the arsenal of available degradation techniques.

5. Conclusion

The possibility of using SECM as a local and accelerated degradation technique on nano-composite silicon-nanostructure-con-ducting polymer electrodes was investigated and compared to the results from conventional degradation methods. It showed that SECM can be used not only as a powerful analytical technique to access the kinetics parameters of conductive polymers such as PEDOT:PSS but also as a local degradation technique. Degradation by SECM shows similar results to those found in the literature for the Si Wafer-conducting polymer and SiNWs-conducting polymer. However, the SiNTrs-conducting polymer electrodes showed a degradation behavior never observed before on nano-composite polymer electrodes. Two parallel degradation mechanisms were successfully identified, involving both the silicon-based nanostructures and the conducting polymer matrix. The degradation method using SECM was also proven to be faster than any known degradation method so far at the microscopic scale. The possibility to act at the local scale makes SECM an efficient technique for the study of conducting polymers. Our ambition with this paper is not to replace but to complement other techniques of analysis and degradation of electrodes with a fast, local, and cheap asset.

Acknowledgements

This work was supported by the French Government (L'Agence Nationale de la Recherche [ANR] - 19-ASTR-0026-01 program, ECOPE project).

References

[1] A. V. Volkov, K. Wijeratne, E. Mitraka, U. Ail, D. Zhao, K. Tybrandt, J. W. Andreasen, M. Berggren, X. Crispin, I. V. Zozoulenko, Adv. Funct. Mater. 2017, 27, 1700329.

[2] Z. Peng, X. Liu, H. Meng, Z. Li, B. Li, Z. Liu, S. Liu, ACS Appl Mater Interfaces 2017, 9, 4577.

[3] C. Kim, D. Y. Kang, J. H. Moon, Nano Energy 2018, 53, 182.

[4] H. Shi, C. Liu, Q. Jiang, J. Xu, Adv. Electron. Mater. 2015, 1, 1500017.

[5] J. Park, H. Yoon, G. Kim, B. Lee, S. Lee, S. Jeong, T. Kim, J. Seo, S. Chung, Y. Hong, Adv. Funct. Mater. 2019, 29, 1902412.

[6] L. Yan, X. Gao, J. P. Thomas, J. Ngai, H. Altounian, K. T. Leung, Y. Meng, Y. Li, Sustainable Energy Fuels 2018, 2, 1574.

[7] P. Kumar, Conducting Polymer and Natural Molecular Materials for Bioelectronics and Energy Strorage, Université de Montréal, 2016.

[8] G. Wang, L. Zhang, J. Zhang, Chem. Soc. Rev. 2012, 41, 797.

[9] L. Qin, Q. Tao, A. El Ghazaly, J. Fernandez-Rodriguez, P. O. Å. Persson, J. Rosen, F. Zhang, Adv. Funct. Mater. 2018, 28, 1703808.

[10] Y. Li, G. Ren, Z. Zhang, C. Teng, Y. Wu, X. Lu, Y. Zhu, L. Jiang, J. Mater. Chem. 2016, 4, 17324.

[11] D. Aradilla, G. Bidan, P. Gentile, P. Weathers, F. Thissandier, V. Ruiz, P. Gómez-Romero, T. J. S. Schubert, H. Sahin, S. Sadki, RSC Adv. 2014, 4, 26462.

[12] A. Valero, A. Mery, D. Gaboriau, P. Gentile, S. Sadki, ACS Appl. Energy Mater. 2019, 2, 436.

[13] R. Mažeikienė, A. Malinauskas, Synth. Met. 2001, 123, 349.

[14] K. Rasmussen, G. Grampp, M. Van Eesbeek, T. Rohr, ACS Appl. Mater. Interfaces 2010, 2, 1879.

[15] S. Bontapalle, S. Varughese, Polym. Degrad. Stab. 2020, 171, 109025.

[16] S. R. Dupont, F. Novoa, E. Voroshazi, R. H. Dauskardt, Adv. Funct. Mater. 2014, 24, 1325.

[17] E. Vitoratos, S. Sakkopoulos, E. Dalas, N. Paliatsas, D. Karageorgopoulos, F. Petraki, S. Kennou, S. A. Choulis, Org. Electron. 2009, 10, 61.

[18] C. Duc, G. G. Malliaras, V. Senez, A. Vlandas, Synth. Met. 2018, 238, 14.

[19] H. Bülter, F. Peters, G. Wittstock, Energy Technol. 2016, 4, 1486.

[20] B. Tao, L. C. Yule, E. Daviddi, C. L. Bentley, P. R. Unwin, Angew. Chem., Int. Ed. 2019, 58, 4606.

[21] A. Sumboja, U. M. Tefashe, G. Wittstock, P. S. Lee, Adv. Mater. Inter-faces 2015, 2, 1400154.

[22] M. Tsionsky, A. J. Bard, D. Dini, F. Decker, Chem. Mater. 1998, 10, 2120.

[23] M. Arca, M. V. Mirkin, A. J. Bard, J. Phys. Chem. 1995, 99, 5040.

[24] M. Burgess, K. Hernández-Burgos, B. H. Simpson, T. Lichtenstein, S. Avetian, G. Nagarjuna, K. J. Cheng, J. S. Moore, J. Rodríguez-López, J. Electrochem. Soc. 2016, 163, H3006.

[25] T. Okajima, T. Ohsaka, N. Oyama, J. Electroanal. Chem. 1991, 315, 175.

[26] R. Cornut, C. Lefrou, J. Electroanal. Chem. 2008, 621, 178.

[27] D. Gaboriau, D. Aradilla, M. Brachet, J. Le Bideau, T. Brousse, G. Bidan, P. Gentile, S. Sadki, RSC Adv. 2016, 6, 81017.

[28] P. Gentile, T. David, F. Dhalluin, D. Buttard, N. Pauc, M. Den Hertog, P. Ferret, T. Baron, Nanotechnology 2008, 19, 125608.

[29] F. Thissandier, L. Dupré, P. Gentile, T. Brousse, G. Bidan, D. Buttard, S. Sadki, Electrochim. Acta 2014, 117, 159.

[30] F. Oehler, P. Gentile, T. Baron, P. Ferret, M. Den Hertog, J. Rouviére, Nano Lett. 2010, 10, 2335.

[31] P. Gentile, A. Solanki, N. Pauc, F. Oehler, B. Salem, G. Rosaz, T. Baron, M. Den Hertog, V. Calvo, Nanotechnology. 2012, 23, 215702.

[32] Y. Wang, J. G. Limon-Petersen, R. G. Compton, J. Electroanal. Chem. 2011, 652, 13.

[33] H. Ur Rehman, A. Shuja, M. Ali, I. Murtaza, H. Meng, J. Energy Storage2020, 28, 101243.[34] O. Bohlen, J. Kowal, D. U. Sauer, J. Power Sources 2007, 172, 468.

[35] D. J. Yun, J. Jung, Y. M. Sung, H. Ra, J. M. Kim, J. G. Chung, S. Y. Kim, Y. S. Kim, S. Heo, K. H. Kim, Y. J. Jeong, J. Jang, Adv. Electron. Mater. 2020, 6, 2000620